Journal of Innovative Optical Health Sciences
Vol. 6, No. 4 (2013) 1350047 (7 pages)

DOI: 10.1142/S1793545813500478

IMPACT OF DYNAMICAL HYDRATION SHELL AROUND HA PROTEIN ON NONLINEAR CONCENTRATION DEPENDENT T-RAYS ABSORPTION

YIWEN SUN*,‡, TIANFU WANG*, SIPING CHEN*, JIAN ZUO†,
ZHENWEI ZHANG† and CUNLIN ZHANG†
*National-Regional Key Technology Engineering Laboratory
for Medical Ultrasound
Guangdong Key Laboratory for Biomedical Measurements
and Ultrasound Imaging
Department of Biomedical Engineering
School of Medicine, Shenzhen University
Shenzhen 518060, P. R. China

†Department of Physics, Capital Normal University
Beijing 100037, P. R. China
‡ywsun@szu.edu.cn

Received 27 July 2013
Accepted 10 September 2013
Published 22 October 2013

T-rays is sensitive to covalently cross-linked proteins and can be used to probe unique dynamic properties of water surrounding a protein. In this paper, we demonstrate the unique absorption properties of the dynamic hydration shells determined by hemagglutinin (HA) protein in terahertz frequency. We study the changes arising from different concentrations in detail and show that nonlinear absorption coefficient is induced by the dynamic hydration water. The binary and ternary component model were used to interpret the nonlinearity absorption behaviors and predict the thickness of the hydration shells around the HA protein in aqueous phase.

Keywords: T-rays; absorption coefficient; hemagglutinin; hydration shell.

1. Introduction

T-rays, also called terahertz (THz) radiation, THz waves or THz light, is a region of the electromagnetic spectrum (EM) between far-infrared and microwaves. The T-rays region is typically defined as ranging from 0.1 to 10 THz (1 THz = 10^{12} Hz) in frequency, or 3 mm to 30 μm in wavelength.[1] This radiation has very low photon energy and thus it

will not cause harmful ionization in biological tissues; this makes it very attractive for medical applications. The vibrational modes corresponding to protein tertiary structural motion lie toward the far-infrared end of the T-rays range: the molecular properties that can be probed at these frequencies sensitively include bulk dielectric relaxation modes, phonon modes and intermolecular vibrations.[2–4] Influenza remains a major medical problem and is a constant threat to human health. Influenza virus hemagglutinin (HA) is a glycoprotein integral to the influenza virus envelope. HA is involved in two major functions: recognition of target cells, by binding to their sialic acid-containing receptors, and fusion of the viral and the endosomal membranes succeeding endocytosis.[5] However, biological proteins often require an aqueous phase in order to be transported to their target sites. Proteins influence both the spatial and dynamic arrangement of neighboring liquid layers through weak intermolecular interactions.[6] Understanding the structure and dynamics of HA in solutions is essential for designing novel antiviral agents that can potentially inhibit its binding or fusogenic activities. Thus, we investigate whether the THz absorption properties of HA proteins are affected by the presence of the dynamical hydration shell around HA to determine if THz spectroscopy could potentially be used for label-free influenza virus detection in future.

2. Experimental Methods

Spectra in the T-rays region were acquired using a commercial Z-3™ Time Domain THz spectrometer (Zomega THz Corp., Troy, USA).[7] In this system, optical excitation is achieved by a mode-locked Mai-Tai laser which emits less than 120 fs pulses centered at a wavelength of 800 nm, with a 80 MHz repetition rate and an average power of ∼1W. The measurements were conducted in the typical transmission geometry because data showed fewer artifacts (such as etalon and first surface reflection interference). The THz-TDS works at room temperature (∼298 K), the optics are purged using nitrogen gas to remove the water vapor from the air to decrease the humidity down to less than 1%. The usable frequency range is from about 0.1 to 2.5 THz but the valid range tends to decrease when the sample is in aqueous phase due to signal attenuation by the sample.

Our selected protein, Recombinant Influenza A Virus H9N2 HA protein (Sino Biological, Inc.), is a DNA sequence encoding the extra cellular domain (Met1-Lys523) of the influenza A H9N2 HA (A/Guineafowl/HongKong/WF10/99(H9N2)) which was expressed in human cells, fused with a C-terminal polyhistidine tag. It comprises of 516 amino acids and has a predicted molecular mass of approximately 65–75 kDa band in SDS-PAGE under reducing conditions. PBS (pH 7.4) was used to dilute the original solution to obtain concentrations of 0.43, 0.225, 0.113, 0.056, 0.029, 0.015 and 0.0075 mg/ml. The solutions at room temperature are clear and without precipitates.

The liquid cell was fabricated from TOPAS™ 5013L-10; this material (which is a Cyclic Olefin Copolymer, COC) was chosen as it has very low attenuation at THz frequencies.[8] Moreover, TOPAS™ was chosen over other THz transparent materials because it is chemically inert to the biomaterials.[9,10] Since water strongly attenuates T-rays, the penetration depth of the T-rays into liquid sample is typically less than 500 μm. Therefore, a thin liquid layer in the liquid cell was prepared which is of the order of a few millimeters thick. Furthermore, the thin layer can also avoid unwanted reflections signal from the surface of the sample during the measurement. The gradual difference in the concentration of the protein solutions from 0.0075 to 0.43 mg/ml was calculated and was found ready to be used in tubes. Before each measurement, the liquid cell was cleaned using acetone and then dried at ambient temperature to remove any surface contamination. The hydrated protein formulation was extracted and pipetted into each cell for the THz measurement. Each sample was measured four times. By averaging the spectra, systematic errors produced by wrong positioning, as well as present heterogeneities in the sample, were minimized. The clean homogeneous empty sample cell was also measured as a reference (refractive index ∼1.53) enabling the spectroscopic properties of the sample to be accurately determined.

3. Results and Discussion

3.1. *Liquid cell in transmission geometry*

A typical sample cell geometry used for liquid measurement in transmission system is illustrated in Fig. 1.

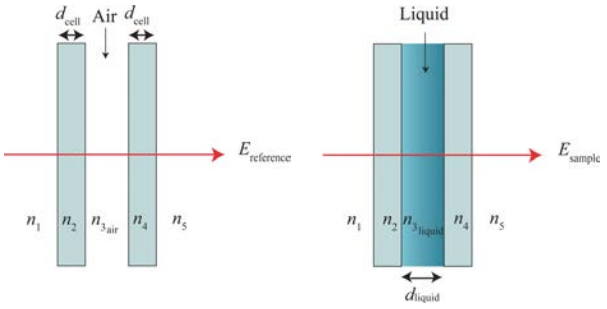

(a) (b)

Fig. 1. Transmission schematics for the liquid sample cell geometry. This schematic illustrates the notation for specifying T-rays radiation propagation through liquid sample, inserted in polymer window cell.

The cell allows for a small volume of solution to reside between the plates. Here, a spacer with a thickness, d_{liquid}, is inserted in between the parallel plates. T-rays radiation is illuminated through the window cells to produce $E_{\text{reference}}$ [see Fig. 1(a)]. For the sample measurements, the air gap with thickness, d_{liquid}, is filled with liquid. Illumination by T-rays radiation through this window cell set up produces E_{sample} [see Fig. 2(b)]. Taking the ratio of $E_{\text{reference}}$ and E_{sample} gives the complex transmission coefficient $T(\omega)$ as follows:

$$\tilde{T}(\omega) = \frac{\tilde{n}_{3_{\text{liquid}}}(\tilde{n}_2+1)^2}{(\tilde{n}_2+\tilde{n}_{3_{\text{liquid}}})^2} \exp\left(\frac{-i\omega d_{\text{liquid}}}{c}(\tilde{n}_{3_{\text{liquid}}}-1)\right), \tag{1}$$

where the complex refractive index of the window cell is $\tilde{n}_2 = \tilde{n}_4$. The refractive index of air is denoted as $\tilde{n}_1 = \tilde{n}_5 = \tilde{n}_{\text{air}} = 1$. Here, $\tilde{n}_3$ liquid is the complex refractive index of the liquid. With the above assumption, the analytic expression for the THz material parameters can be found with some approximation given in Duvillaret *et al.*[11] Substituting the complex refractive index, $\tilde{n}_{3_{\text{liquid}}} = n_{3_{\text{liquid}}} - i\kappa_{3_{\text{liquid}}}$ into Eq. (1) reveals the frequency-dependent magnitude:

$$\rho(\omega) = \frac{n_{3_{\text{liquid}}}(\omega)(n_2+1)^2}{(n_2+n_{3_{\text{liquid}}}(\omega))^2} \exp\left(-\frac{\omega d_{\text{liquid}}}{c}\kappa_{3_{\text{liquid}}}(\omega)\right). \tag{2}$$

The frequency-dependent refractive index can be simplified and expressed as,

$$n_{3_{\text{liquid}}}(\omega) = \frac{\phi(\omega)c}{\omega d_{\text{liquid}}} + 1. \tag{3}$$

The parameter $\phi(\omega)$ is the frequency-dependent phase extracted from Eq. (1). The frequency-dependent extinction coefficient can be obtained by rearranging Eq. (2). Thus, the extinction coefficient can be expressed as

$$\kappa_{3_{\text{liquid}}}(\omega) = -\frac{c}{\omega d_{\text{liquid}}} \times \ln\left[\rho(\omega)\frac{(n_2+n_{3_{\text{liquid}}}(\omega))^2}{n_{3_{\text{liquid}}}(\omega)(n_2+1)^2}\right]. \tag{4}$$

The frequency-dependent absorption coefficient can be written as follows:

$$\alpha_{\text{liquid}}(\omega) = 2\frac{\kappa_{3_{\text{liquid}}}(\omega)\omega}{c}. \tag{5}$$

One may rewrite Eq. (4) with (5) as follows:

$$\alpha_{\text{liquid}}(\omega) = -\frac{2}{d_{\text{liquid}}} \times \ln\left[\rho(\omega)\frac{(n_2+n_{3_{\text{liquid}}}(\omega))^2}{n_{3_{\text{liquid}}}(\omega)(n_2+1)^2}\right]. \tag{6}$$

In Fig. 2, we show the typical T-rays waveform of the reference pulse (red line) and sample pulse (blue line). The fast Fourier transformation of the electric fields in the time-domain (Fig. 2(a)) yields the frequency-domain spectral (Fig. 2(b)).

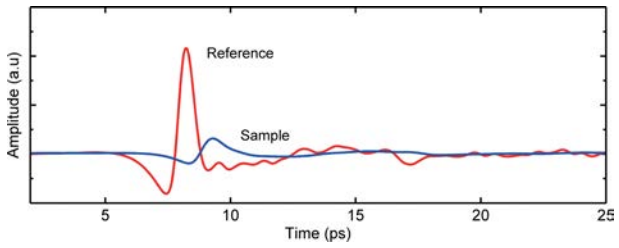

(a)

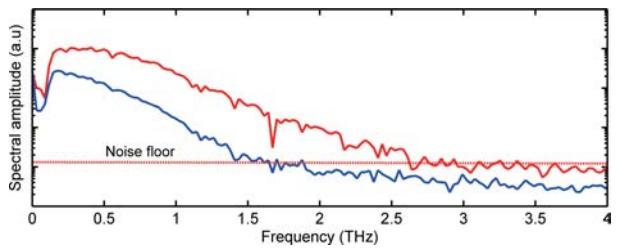

(b)

Fig. 2. Typical temporal waveform and frequency spectral for a reference and a sample signal. A bandwidth of up to 1.6 THz is obtained from our experimental setup.

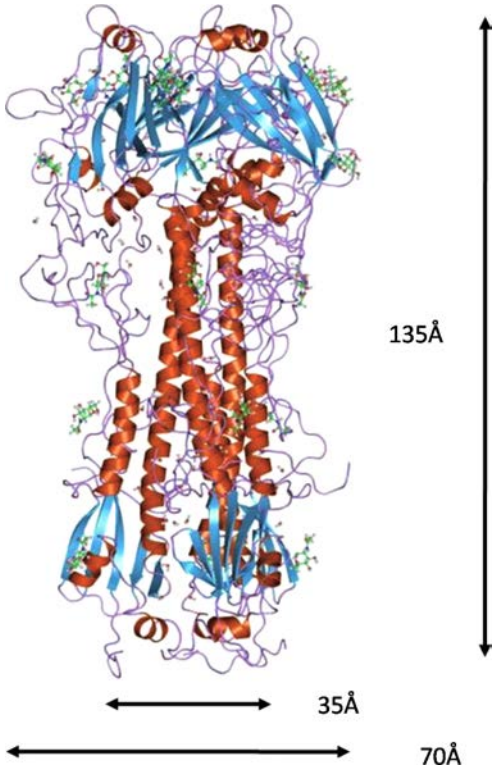

Fig. 3. The trimeric structure of HA protein.

According to the frequency spectral, a bandwidth of approximately 1.6 THz is achieved in our setup configuration.

3.2. *Concentration-dependent measurements*

The published X-ray crystal structure of HA protein indicates a cylinder-shaped trimer ∼135 Å long, varying between 35 and 70 Å along the radial direction[12] as shown in Fig. 3. Theoretically, a small particle is subject to the random wandering of Brownian motion. Thus, the aquatic HA proteins obey the laws of diffusion in their approach to another particles. Diffusion transport depends on diffusivity of the solute and the transport rate for a cylinder model which is given by Eq. (7)[13]:

$$J_c = 2\pi d_s D_v V \left[0.52\left(\frac{L}{d}\right)^{-0.33} + 0.45\left(\frac{L}{d}\right)^{0.43}\right], \tag{7}$$

where d is the cylinder's diameter, L is the length of cylinder, D_v and V represent the diffusivity constant and the concentration of the protein and d_s is the volume-equivalent spherical diameter. The

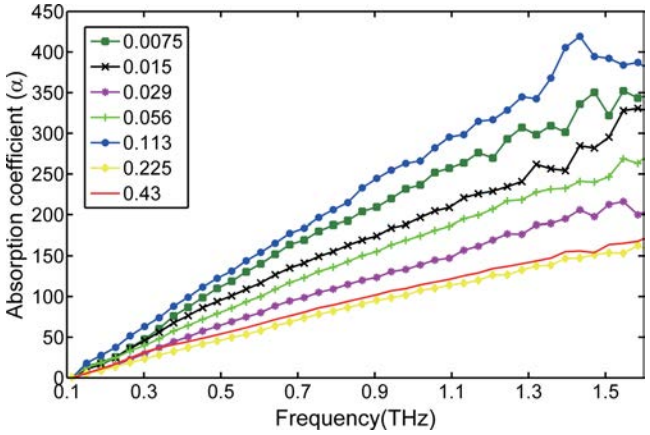

Fig. 4. T-rays absorption coefficients of HA protein in solution at concentrations from 0.0075 to 0.43 mg/ml.

effect of shape (L/d) relative to that of a sphere of the same volume is given by the factor within the square brackets. Following Eq. (7) we can see that particle shape does not greatly affect its transport rate in the solutions, hence we assume that HA protein can be considered as a spherical particle in all subsequent dynamic analysis.

Figure 4 shows the concentrations dependence of the absorption coefficients of HA protein in solution. T-rays absorption spectra are very sensitive to crystalline structures,[14,15] but the liquid protein form of HA lacked any distinct peaks in the spectral region studied. To get a full picture of how the absorption coefficient depends on both frequency and concentration, we have drawn a 3D plot in Fig. 5. Although the differences on the absorption coefficients differ for these frequencies, the overall variation in the absorption with concentration presents the same trend. We extracted the concentration dependence absorption of HA protein in

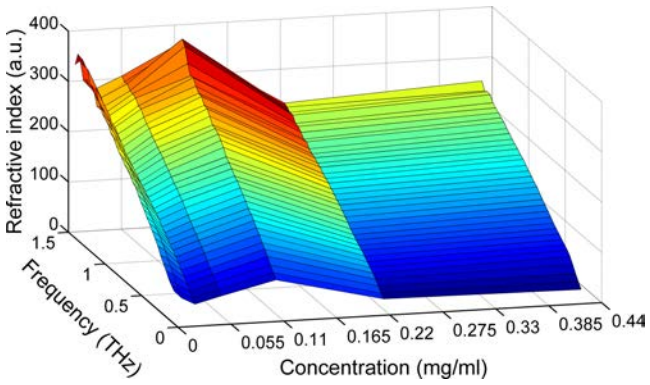

Fig. 5. Difference in the T-rays absorption coefficient against HA protein concentration from 0.15 to 1.50 THz.

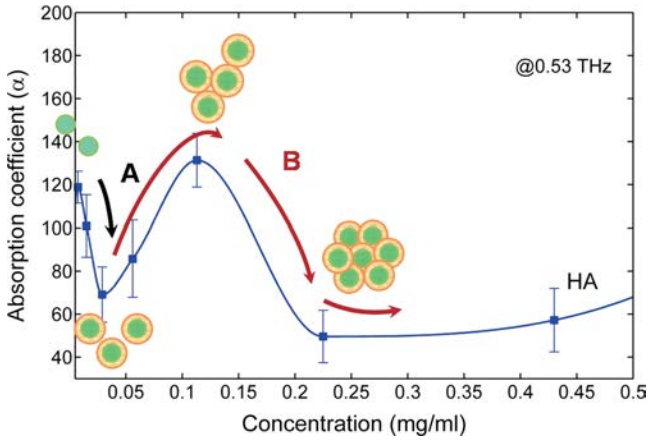

Fig. 6. Schematic diagram for overlap of the hydration shells to interpret the nonlinear absorption behaviors depends on the HA concentration using a binary component model (A) and a ternary component model (B).

buffer solutions at 0.53 THz as shown in Fig. 6 for further description. The 95% confidence intervals are plotted as error bars to determine whether differences are statistically significant.

In concept, T-rays absorption coefficient $\alpha_{\text{ideal}}(\omega)$ is a linear function with increasing protein concentration in the solvent volume V based on Beer–Lambert law. As expected, the proteins were much less absorbing than the buffer solution and so the absorption coefficient decreased with increasing protein concentration. We used Eq. (8)[16] for the absorption coefficient of an ideal mixture. This equation is based on the two-component excluded volume model and was used to fit absorption coefficient versus protein concentration.

$$\alpha_{\text{ideal}}(\omega) = A_1\alpha_{\text{protein}}(\omega) + A_2\alpha_{\text{solvent}}(\omega), \qquad (8)$$

where α_i is the absorption coefficient for each component, and the coefficient $A_1 = V_{\text{protein}}/V$ and $A_2 = (V - V_{\text{protein}})/V$. In the protein solutions, the absorption of the two-component model which was affected by only the absorption of the buffer and the protein would lead to the linear concentration dependence. Since the protein solutions with low concentration were nearly transparent in the T-rays frequency, a liner decrease of the absorption coefficient with increasing protein concentration in a solvent volume V was indicated. In Fig. 6, at low concentrations from 0.0075 to 0.029 mg/ml, the absorption coefficient decreases with increasing protein concentration, which presents the typical two-component excluded volume model described in Eq. (12). After that, the absorption coefficient increases linearly with protein concentrations up to 0.113 mg/ml and then drops, leading to non-monotonic and nonlinear concentration dependence behaviors which cannot be explained just by a two-component excluded volume model.

The water layer around the protein molecule, which is usually called hydration water, is known to exhibit distinct dynamical properties compared with bulk water. The volume of the hydration water increases with the protein concentration. If the absorbance of the hydration water exceeds the absorbance of the bulk water, the overall absorption coefficient will increase linearly with the protein concentration. Hence, in Fig. 6 after the absorption linearly decreases as described by the binary model, the increasing absorption coefficient can be explained as the contribution of the dynamical hydration shell around the protein molecule. Therefore, we continued our analysis in terms of individually determined absorption coefficients using a ternary component model (protein, hydration water and bulk water), which assumes a distinct absorption coefficient of water around the solute molecule due to distinct properties of the solvation water.[17] In this model expressed by Eq. (9), the ideal absorption coefficient is described as the volume-weighted fraction of the absorption of protein (A_1), the hydration water (A_2) and the bulk water (A_3).

$$\alpha_{\text{ideal}}(\omega) = A_1\alpha_{\text{protein}}(\omega) + A_2\alpha_{\text{hydration\_shell}}(\omega) + A_3\alpha_{\text{bulk\_water}}(\omega). \qquad (9)$$

Note this in Fig. 6, the absorbance of the dynamical hydration shell exceeds the absorbance of the bulk water displaced by the shell and the protein, where the overall absorption beginning at 0.029 mg/ml will at first increase linearly with protein concentration. Then, the turnover at 0.113 mg/ml can be explained as the beginning of overlap of the dynamical hydration shells around the protein molecule. Eventually, the shells get saturated at 0.225 mg/ml such that it is not possible to increase absorbance with increasing concentration.

Hydrogen bond rearrangement in water occurs on the picosecond time scale, which the T-rays spectroscopy can access and directly investigate the hydration layers around the HA proteins. The hydration water around the protein contributes to a dynamical-coupling issue which presents a nonlinear absorption spectrum in the T-rays region. This fundamental work is the first T-rays study of

the dynamical hydration absorption of hydrated HA proteins: it demonstrates the fundamental capabilities of T-rays spectroscopy as well as highlighting that HA has interesting features in the T-rays range. Although the research has its aim, it is perhaps limited to the analysis of T-rays spectra of this system in terms of a binary and a ternary component model. However, the water layer around a biological molecule has been known to exhibit distinct dynamical properties compared with bulk water using relevant experiments,[18] so we continue our analysis in terms of these model with contributions from HA protein, bulk water and hydration water around HA.

According to this model, the absorption coefficient starts to behave nonlinearly at a concentration of 0.113 mg/ml — this is due to hydration shell overlap, and gets saturated at 0.225 mg/ml. We, therefore, use these concentrations for c_{protein} in the formula below to determine limits for the average radius R of the antibody molecule:

$$\frac{4\pi}{3}R^3 = \frac{m_{\text{mass}}}{c_{\text{protein}}N_A}, \tag{10}$$

where m_{mass} is the molecular mass and N_A is the Avogadro constant. The molecular mass of the HA depends on the result of glycosylation, so to determine the upper and lower limits of the radius we also need to consider the highest and lowest possible molecular masses with the lowest and highest concentrations for c_{protein}. These give limits on the average radius for HA of $R_{0.113} = 62.6 \pm 1.5$ Å. Similarly, the average radius for saturated HA is $R_{0.225} = 49.8 \pm 1.2$ Å. From these we can directly deduce the thickness of the hydration shell ($R_{\text{shell}} = R_{0.113} - R_{0.225}$) to be 12.8 ± 1.3 Å for HA protein.[17–19] This result corresponds to about 4 or 5 hydration water shells around a HA protein molecule ($\sim$3 Å average extension per water molecule) which is the similar value that has been reported.[18]

4. Conclusion

In summary, we have used T-rays pulse spectroscopic technology to determine the concentration-dependent absorption coefficient properties of HA protein in solutions. The T-ray absorption spectrum is sensitive to the nonlinear absorption coefficients of the protein molecules due to the dynamic hydration shell around them. The nonlinearity has to be attributed to the onset of overlapping of the hydration layers. Furthermore, using T-rays spectroscopy, we are able to determine the size of the hydration layer on the femtosecond to picosecond time scale. Therefore, we predict that T-rays pulsed spectroscopy could potentially be used for revealing the dynamics of the hydration water which is sensitive to the concentration of proteins. In further work, we will also investigate different dielectric relaxation models for more complex HA antigen–antibody systems in an aqueous phase, so as to understand how to realize the label-free influenza virus detection technology.

Acknowledgment

We gratefully acknowledge partial financial support for this work from the National Natural Science Foundation of China (No. 61205092), Guangdong Natural Science Foundation (No. S2012040007668), Foundation for Distinguished Young Talents in Higher Education of Guangdong, China (No. 2012LYM_0116) and Special Foundation of New Industries Development, Shenzhen (ZDSY201206 12094855904).

References

1. P. H. Siegel, "Terahertz technology in biology and medicine," *IEEE Trans. Microw. Theory Tech* **52**, 2438–2447 (2004).
2. A. Markelz, A. Roitberg, E. J. Heilweil, "Pulsed terahertz spectroscopy of DNA, bovine serum albumin and collagen between 0.06 to 2.00 THz," *Chem. Phys. Lett.* **320**, 42–48 (2000).
3. A. Markelz, S. Whitmire, J. Hillebrecht, R. Birge, "The time domain spectroscopy of biomolecular conformational modes," *Phys. Med. Biol.* **47**, 3797–3805 (2002).
4. B. M. Fischer, M. Walther, P. U. Jepsen, "Far-infrared vibrational modes of DNA components studied by terahertz time-domain spectroscopy," *Phys. Med. Biol.* **47**, 3807–3814 (2002).
5. J. M. White, L. R. Hoffman, J. H. Arevalo, I. A. Wilson, Attachment and entry of influenza virus into host cells. Pivotal roles of hemagglutinin, *Structural Biology of Viruses*, pp. 88–104, Oxford University Press, NY (1997).
6. R. Pethig, "Protein-water interactions determined by dielectric methods," *Annu. Rev. Phys. Chem.* **43**, 177–205 (1992).
7. J. C. Maxwell, *A Treatise on Electricity and Magnetism*, 3rd edition, Vol. 2, pp. 68–73, Clarendon, Oxford (1892).

8. J. Balakrishnan, B. M. Fischer, D. Abbott, "Sensing the hygroscopicity of polymer and copolymer materials using terahertz time-domain spectroscopy," *Appl. Opt.* **48**, 2262–2266 (2009).
9. R. K. Jena, C. Y. Yue, "Cyclic olefin copolymer based microfluidic devices for biochip applications: Ultraviolet surface grafting using 2-methacryloyloxyethyl phosphorylcholine," *Biomicrofluidics* **6** (1), 012822–012822-12 (2012).
10. Y. W. Sun, Z. X. Zhu, D. Abbott, E. Pickwell-MacPherson *et al.*, "Observing the temperature dependent transition of the GP2 peptide using terahertz spectroscopy," *PLoS ONE* **7**(11), e50306 (2012).
11. L. Duvillaret, F. Garet, J. Coutaz, "Highly precise determination of optical constants and sample thickness in terahertz time-domain spectroscopy," *Appl. Opt.* **39**, 409–415 (1999).
12. I. A. Wilson, J. J. Skehel, D. C. Wiley, "Structure of the haemagglutinin membrane glycoprotein of influenza virus at 3 Å resolution," *Nature* **289**, 366–373 (1981).
13. G. Murray, G. A. Jackson, "Viral dynamics: A model of the effects of size, shape, motion and abundance of single-celled planktonic organisms and other particles," *Mar. Ecol. Prog. Ser.* **89**, 103–116 (1992).
14. P. F. Taday, I. V. Bradley, D. D. Arnone, "Terahertz pulse spectroscopy of biological materials: L-glutamic acid," *J. Biol. Phys.* **29**, 109–115 (2003).
15. P. F. Taday, I. V. Bradley, D. D. Arnone, M. Pepper, "Using terahertz pulse spectroscopy to study the crystalline structure of a drug: A case study of the polymorphs of ranitidine hydrochloride," *J. Pharm. Sci.* **94**, 831–838 (2003).
16. T. Tassaing, Y. Danten, M. Besnard, E. Zoidis, J. Yarwood, "A far infrared study of benzene-fluorinated benzene binary mixtures," *Chem. Phys.* **184**, 225–231 (1994).
17. J. K. Seung, "Studies of protein-protein and protein-water interactions by small angle x-ray scattering, terahertz spectroscopy, asmos, and computer simulation," Ph.D. Thesis, University of Illinois at Urbana-Champaign, Illinois (2008).
18. U. Heugen, G. Schwaab, E. Brundermann, M. Heyden, X. Yu, D. M. Leitner, M. Havenith, "Solute-induced retardation of water dynamics probed directly by terahertz spectroscopy," *Proc. Natl. Acad. Sci. USA* **103**, 12301–12306 (2006).
19. Y. W. Sun, Y. T. Zhang and E. Pickwell-MacPherson, "Investigating antibody interactions with a polar liquid using terahertz pulsed spectroscopy," *Biophys. J.* **100**, 225–231 (2011).